Journal of Cleaner Production 265 (2020) 121792

Contents lists available at ScienceDirect

Journal of Cleaner Production

journal homepage: www.elsevier.com/locate/jclepro

Grid-scale agricultural land and water management: A remote-sensing-based multiobjective approach

Yikuan Tang [a, b], Fan Zhang [a, b], Bernard A. Engel [c], Xiao Liu [a, b], Qiong Yue [a, b], Ping Guo [a, b, *]

[a] *Center for Agricultural Water Research in China, China Agricultural University, Beijing, 100083, China*
[b] *Wuwei Experimental Station for Efficient Water Use in Agriculture, Ministry of Agriculture and Rural Affairs, Wuwei, 733000, China*
[c] *Department of Agricultural and Biological Engineering, Purdue University, West Lafayette, IN, 47907, USA*

ARTICLE INFO

Article history:
Received 27 January 2020
Received in revised form
15 April 2020
Accepted 17 April 2020
Available online 23 April 2020

Keywords:
Remote-sensing-based multiobjective approach
Downscaling
Agricultural land and water planning
Sustainable development of agriculture

ABSTRACT

This paper developed a remote-sensing-based multiobjective (RSM) approach to formulate sustainable agricultural land and water resources management strategies at a grid scale. To meet the spatial resolution and accuracy need of agricultural management, downscaled precipitation data sets were obtained with the help of global precipitation measurement (GPM) data and other spatial information. Spatial crop water requirement information were obtained via the combination use of the Penman-Monteith method, remote sensing information (MOD16/PET) and virtual water theory. Through integrating these spatial data and considering the impact of different spatial environments on crop growth, a grid-based integer multiobjective programming (GIMP) model was developed to determine best suitable crop planting types at all grids. GIMP can simultaneously consider several conflicting objectives: crop growth suitability, crop spatial water requirements, and ecosystem service value. Further, GIMP results were inputted into a grid-based nonlinear fractional multiobjective programming (GNFMP) model with three objectives: maximize economic benefits, maximize water productivity, and minimize blue water utilization, to optimize irrigation-water allocation. To verify the validity of the proposed approach, a real-world application in the middle reaches of Heihe River Basin, northwest China was conducted. Results show that the proposed method can improve the ecosystem service value by 0.36 $\times$ 10^8 CNY, the economic benefit by 21.85%, the irrigation-water productivity by 25.92%, and reduce blue water utilization rate by 24.32% comparing with status quo.

1. Introduction

Global economic development and population growth jointly deepen the water shortage and environmental crisis, which is an urgent global problem facing humankind. Agriculture is the largest water consumer and one of the major leading sources of environmental degradation (Zhang et al., 2019b). The limited agricultural land and water resources are the major constraint on agricultural production, which calls for more efficient resource utilization strategies. Mathematical optimization models have been proved as important tools in optimally allocating limited agricultural land (Gui et al., 2016) and water resources (Li et al., 2019a), maintaining ecological health (Zhang et al., 2019b) and supporting sustainable development of regional agriculture (Li et al., 2019b). When dealing with real-world problems, some basic parameters, such as precipitation and evapotranspiration (*ET*), have high spatiotemporal variability (Tang et al., 2019), increasing the difficulty in modeling. The emergence of remote sensing technology produces more spatial information (Michaelides et al., 2009), and brings hope to solve the above problems (Bastiaanssen et al., 2000). It is a hot issue to make full use of remote sensing information in optimizing management of agricultural spatial resources for improving the utilization efficiency of limited resource. Therefore, a remote-sensing-based multiobjective (RSM) approach is necessary for determining crop planting type and allocating limited irrigation-water to spatial grids (1 km $\times$ 1 km) with the help of remote sensing information.

Precipitation and *ET* play a very important role in the management of agricultural land and water resources. Especially for some arid and semi-arid regions, there is strong spatial variability and temporal distribution in precipitation and *ET*, which need to be

* Corresponding author. Center for Agricultural Water Research in China, China Agricultural University, Tsinghuadong Street No. 17, Beijing, 100083, PR China.
E-mail address: guop@cau.edu.cn (P. Guo).

https://doi.org/10.1016/j.jclepro.2020.121792
0959-6526/

considered in decision-making processes (Tang et al., 2019). In recent years, the global precipitation measurement (GPM, Huffman et al., 2019) data with higher spatial resolution (0.1°), time resolution (30 min), and higher accuracy in arid and semi-arid regions was widely used around the world. However, spatial resolution and accuracy of GPM data is too coarse to meet the requirements of RSM approach. Many efforts have been made to downscaling the GPM data, and many factors were considered, such as geographic location information (longitude, latitude) and topographical data (slope, aspect, elevation, Chen et al., 2017). Agnew and Palutikof (2000) attempted to improve the accuracy of precipitation by using multivariate regression with the interpolation of residuals, but remote sensing data were ignored. Previous research developed a downscaling method of spatial sharpening based on multivariate data (Immerzeel et al., 2009). Therefore, this paper attempts to use multivariate linear regression with the residual correction (MLRR) method to obtain down-scaled precipitation data with high accuracy based on GPM data, terrain factors, and geographic location information. Thereafter, the obtained spatial distribution precipitation was evaluated by a cross-validation method (Goovaerts, 2000). As for another key parameter in agricultural production planning, *ET* information from remote sensing has high noise and uncertainty (Velpuri et al., 2013). To address this problem, Tang et al. (2019) developed a new method combining the FAO Penman-Monteith (PM, Allen et al., 1998) method with remote sensing MOD16/PET data (Mu et al., 2007), to obtain more accurate spatial reference evapotranspiration (ET_0). This study further attempts to transfer the spatial ET_0 information to spatial crop water requirement (CWR, Allan, 1993) and crops virtual water content (*VWC*, Su et al., 2014) through virtual water theory (Hoekstra, 2011). These spatial information can be used to formulate more sustainable agricultural production strategies in optimization models.

Complexities in agricultural production systems, such as nonlinear relationships (Fasakhodi et al., 2010), multiple conflicting objectives (Li et al., 2019d), socio-economic conditions (Li et al., 2019a) and environment impacts (Zhang et al., 2019b), were attempted to solve. In agricultural resources management, major tasks are to determine the type of crops and water allocation in specific spatial locations. Thus, mixed 0–1 integer programming was developed to obtain crop-planting structure on cropping plots (Chono et al., 2012). When determining the crop planting structure, crop suitability should be considered due to its high spatial variability, which is an important indicator for evaluating the situation of crop growth environments (such as soil, terrain, and climate, Abah and Petja, 2017). Spatiotemporal variability of CWR and precipitation in different spatial locations should also be taken into consideration in planning agricultural production strategies. Therefore, a grid-based integer multiobjective programming (GIMP) integrated integer 0–1 programming and multiobjective programming was developed to obtain the crop planting structure at a grid scale, which can consider crop growth suitability, spatial *CWR*, and ecosystem service value simultaneously. For water management, some efforts have been made to allocate agricultural water resources, such as Zhang et al. (2018). However, few of them can conduct nonlinear, multiobjective, and fractional problem in planning water allocation at a grid-scale with the help of a spatial crop planting structure, and thus these optimization schemes without spatial location information cannot provide managers precise water allocation schemes in each grid. To address such a problem, this paper further establishes a grid-based nonlinear fractional multiobjective programming (GNFMP) model considering multiple objectives, including economic benefits, irrigation-water productivity, and blue water utilization efficiency at the same time. To generate satisfactory results from the proposed models, the minimum deviation method (Li et al., 2019b) is considered as a possible solution method in dealing with the GIMP and GNFMP model.

In this study, a RSM approach was developed to improve the spatial resolution of agricultural resource management schemes and ensure sustainable agricultural management, which has the following advantages: 1) some key factors with high spatial variability can be obtained based on remote sensing information; 2) the optimal crop planting type can be determined at each grid by the GIMP model considering resources, efficiency and environmental factors; and 3) the corresponding water-allocation schemes based on GIMP results can be calculated through GNFMP considering conflicting objectives.

2. Development of methodology

2.1. Overview of the problem

Modern agriculture advocates a green, efficient and sustainable way to use limited land and water resources. However, the spatial resolution of existing research about land and water resources optimization cannot meet the precise management requirements in real production. For example, most previous management schemes cannot determine crop planting type and irrigation-water in specific spatial locations inside a river basin or irrigation area. In order to provide more practical decision support information, river basin managers urgently need more precise optimization results to manage agricultural production. Recently, the monitoring development of remote sensing in ground precipitation and evapotranspiration provide possible inputs for a RSM approach, but these spatial data always need to be processed to meet managers' requirements. When managing land resources, excessively pursuing economic benefits may cause degradation of the ecological environment, excessive use of blue water resources, and reduce the value of the total ecosystem services. Thus, to use land and water resources in a more efficient and sustainable way, decision makers are facing the following issues. 1) How to determine which crops are most suitable to plant on each spatial grid? A reasonable planting location can not only improve crop yield and quality, but also improve water use efficiency. 2) Due to different potential evapotranspiration and precipitation amounts in different spatial grids, how can requirements for blue water resources be reduced through management measures? 3) How can grain yield, water use efficiency and total system benefits be simultaneously guaranteed? Especially for arid and semi-arid areas, water managers have to not only consider the utilization efficiency and production efficiency of blue water, but also pay attention to farmers' pursuit of economic benefits.

Therefore, the framework developed in this study (Fig. 1) attempts to solve these problems, and can be divided into four parts. 1) Acquisition and processing of basic spatial data. 2) Establishing a GIMP model for optimal spatial crop planting structure at grid scale. 3) Formulating a GNFMP model to obtain spatial irrigation-water allocation. 4) Application of the proposed approach to a real-world case study for improving land and water use efficiency.

2.2. Spatial analysis of basic data

2.2.1. Spatial analysis of precipitation

Some key factors, such as terrain factors (slope, aspect), geographical location information (latitude, longitude) and GPM data are integrated to obtain monthly precipitation results with higher spatial resolution and accuracy. The specific steps of the MLRR method are listed as follows.

(1) Pre-processing

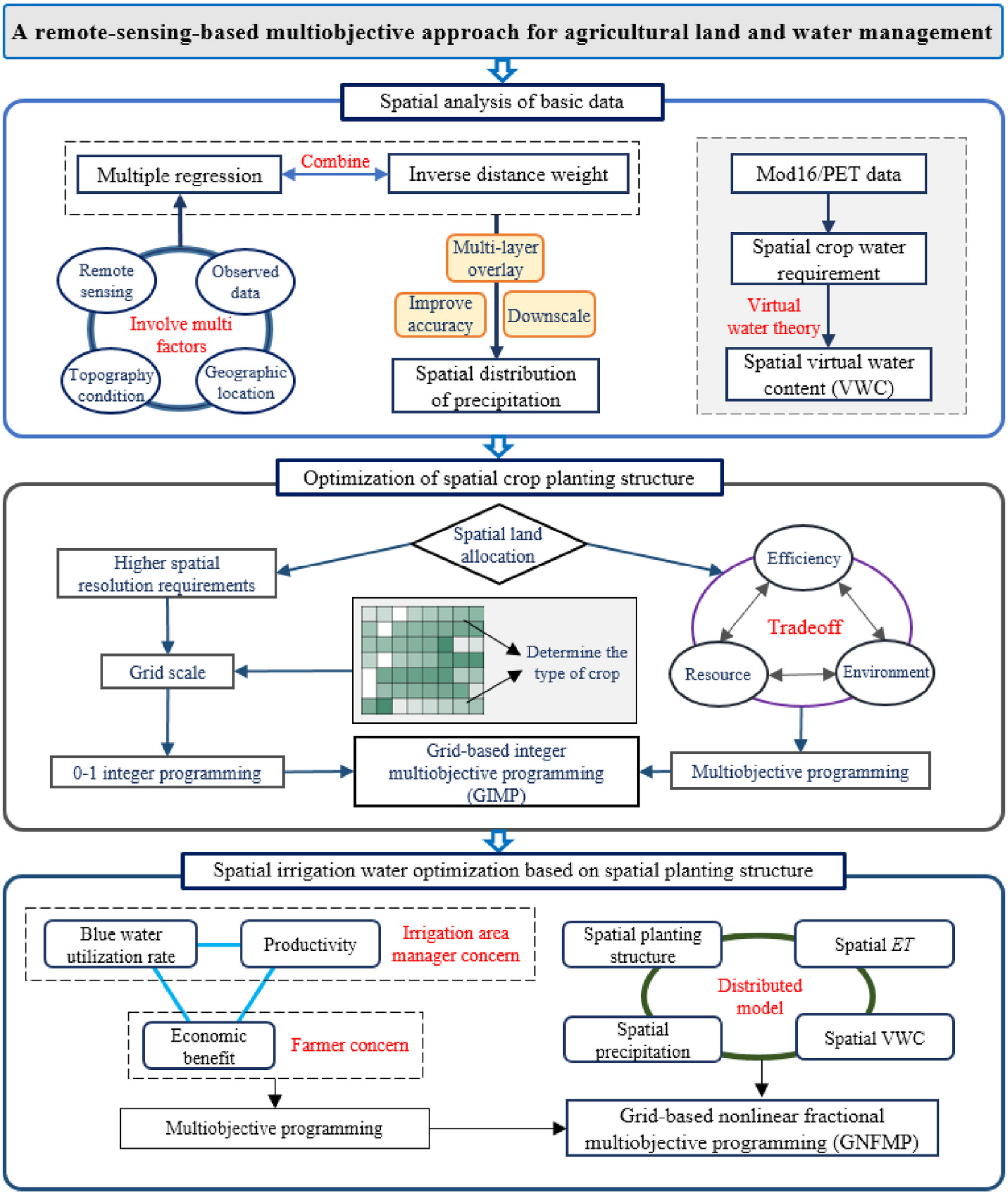

Fig. 1. Framework of the grid-based precise optimization approach.

Use projection transformation, resampling and spatial modeling to process the monthly GPM data, slope and aspect data, and then remove invalid values to obtain these data with a spatial resolution of 1 km in the WGS-1984 coordinate system.

(2) Multiple linear regression

The multiple linear regression (MLR) method is used for downscaling the spatial data, and the typical form can be shown as follows.

$$Y = a_0 + a_1X_1 + a_2X_2 + a_3X_3 + a_4X_4 + a_5X_5 + a_6X_6 \quad (1)$$

Where Y is the precipitation value of meteorol$Y = a_0 + a_1X_1 + a_2X_2 + a_3X_3 + a_4X_4 + a_5X_5 + a_6X_6$ogical stations; X_1, X_2, X_3, X_4, X_5, X_6 represent the monthly normalized value of GPM, DEM, latitude, longitude, aspect, and slope of the meteorological station, respectively; $a_0, a_1, a_2, a_3, a_4, a_5, a_6$represent the regression coefficients, respectively.

The regression results of each grid can be obtained by the following function.

$$Y_j = a_0 + a_1X_{1j} + a_2X_{2j} + a_3X_{3j} + a_4X_{4j} + a_5X_{5j} + a_6X_{6j} \quad (2)$$

Where Y_j is the regression results of the jth grid; X_{1j}, X_{2j}, X_{3j}, X_{4j}, X_{5j}, X_{6j} represent the monthly normalized value of GPM, DEM, latitude, longitude, aspect, and slope of the jth grid.

(3) Inverse distance weighting

Calculating residuals between obtained values from the MLR method and observed results from ground meteorological stations. The IDW method for spatially interpolating the residuals can be shown as follows.

$$R_j = \frac{\sum_{i=1}^{n} \frac{Z_i}{d_i^p}}{\sum_{i=1}^{n} d_i^p} \quad (3)$$

Where R_j is the residual value of the jth grid, Z_i is the residual of the ith meteorological station, n is the number of stations, d_i is the distance from the jth grid to the ith meteorological station, p is the power of distance.

(4) Precipitation downscaling results

The final precipitation of each grid will be obtained as follows:

$$P_j = \mathrm{Y}_j + R_j \quad (4)$$

Where P_j is the precipitation of the jth grid, Y_j is the multiple regression results of the jth grid, R_j is the residual of the jth grid.

(5) Validation

The cross-validation method (Goovaerts, 2000) is used for measuring the applicability of the MLRR method by comparing with GPM data, linear regression (LR), MLR, and IDW method. Thus, root mean square error (*RMSE*), mean absolute error (*MAE*), and mean relative error (*MRE*) are used for the criteria to evaluate different methods. Equations of these indicators are shown as follows.

$$RMSE = \sqrt{\frac{\sum_{i=1}^{N}(P_i - M_i)^2}{N}} \ldots MAE = \frac{\sum_{i=1}^{N}|P_i - M_i|}{N} \ldots MRE = \frac{1}{N}\sum_{i=1}^{N}\left|\frac{ABS(P_i - M_i)}{P_i}\right| \quad (5)$$

Where, P_i is the i th estimated result, M_i is the i th observation result, N is the number of samples.

2.2.2. Spatial analysis of evapotranspiration and VWC

To obtain spatial evapotranspiration and *VWC*, meteorological data from meteorological stations are used for estimating ET_0 through the PM equation. Then, the results obtained can be fitted by monthly MOD16/PET remote sensing data to calculate the spatial ET_0 information of all grids (Tang et al., 2019). Based on information obtained, the monthly *VWC* can be generated. The detailed steps are shown as follows.

(1) Spatial ET_0

PM equation is used for calculating ET_0 (PM results), which can be assumed as the real value of ET_0. According to previous research, MOD16/PET can be converted to ET_0 through the following function.

$$ET_0 = f(PET_{MOD16}) \quad (6)$$

(2) Crop water requirements

CWR are the main reference when formulating optimization models to guide water allocation (Caselles et al., 1992), and can be calculated by the following formula (Westerhoff, 2015):

$$ET_c = K_c \times ET_0 \quad (7)$$

Where, ET_C is the crop water requirement, mm; K_C is the crop coefficient; ET_0 is the spatial reference crop evapotranspiration, mm.

(3) Virtual water content (*VWC*)

The crop *VWC* can be calculated as equation (8) shows (Li et al., 2019b). Thus, the *VWC* value of different crops varies with the crop planting type, spatial location, and time period.

$$VWC = 1,000 \times ET_C \times A \quad (8)$$

Where *VWC* is the virtual water content, m^3; the factor 1,000 is meant to convert the ET_C in mm into m; A is the irrigated area, m^2.

The virtual water is further converted into blue water and green water by the following formulas (Li et al., 2019b).

$$VWC_B = 1,000 \times ET_B \times A \quad (9)$$

$$VWC_G = 1,000 \times ET_G \times A \quad (10)$$

Where VWC_B is the monthly blue water component, m^3; VWC_G is the monthly green water component, m^3; ET_G is monthly green water evapotranspiration, mm; ET_B is monthly blue water evapotranspiration, mm. The ET_G (Su et al., 2014) and ET_B (Li et al., 2019b) can be estimated by the CropWat model (Hoekstra et al., 2011).

$$ET_G = \min(ET_C, EP) \quad (11)$$

$$ET_B = W \quad (12)$$

EP is the effective precipitation, mm; and W is the net irrigation-water; if the effective rainfall is greater than or equal to ET_C, W is 0, mm.

2.3. Crop spatial planting structure optimization

The GIMP model is established for allocating limited land resources, which aims to manage tradeoffs among land use efficiency, resources saving, and environmental impacts. In the GIMP model, mixed 0–1 integer programming can determine the type of crops on each grid. The objectives of this model include maximizing crop growth suitability, maximizing the value of ecosystem services, and minimizing the irrigation-water demand. Constraints of the GIMP model can ensure grain yield and economic benefits of farmers. The overall structure of the GIMP model is now discussed. Appendix I lists meanings of the symbols and applies to all of the following functions.

2.3.1. Objectives

(1) Maximize system crop growth suitability

According to planting suitability of different crops in each grid obtained by the evaluation method (He et al., 2018), the objective of maximizing systemic crop growth suitability can be shown as follows.

$$\max F_1 = \sum_{n=1}^{N}\sum_{i=1}^{I} m_{ni}\eta_{ni} \tag{13a}$$

(2) Minimize spatial crop water requirements of system

In order to save limited irrigation-water, it is necessary to minimize the total crop water demand. The objective function can be represented as follows.

$$\min F_2 = \sum_{n=1}^{N}\sum_{i=1}^{I} m_{ni}A\left(\sum_{t=1}^{T} ET_{Cnit} - \sum_{t=1}^{T} EP_{nt}\right) \tag{13b}$$

(3) Maximize ecosystem service value

According to existing research (Zhang et al., 2019b), the regional ecosystem service value is related to the total crop planting area, and the relationship between these two parameters can be characterized by a function. With help of this relationship, the objective of maximizing ecosystem service value can be expressed as follows.

$$\max F_3 = f\left(\sum_{n=1}^{N}\sum_{i=1}^{I} m_{ni}A\right) \tag{13c}$$

2.3.2. Constraints

(1) Suitability constraints:

$$\mathrm{m}_{ni} = 0 \text{ or } 1, \qquad \forall n, i \tag{13d}$$

$$\sum_{i=1}^{I} m_{ni} \leq 1, \quad \forall i, n \tag{13e}$$

(2) Food security constraints:

$$\sum_{n=1}^{N}\sum_{i=1}^{I} m_{ni}AC_i \geq FD\cdot PO,\ \forall i_{grain\ crop} \tag{13f}$$

(3) Economic benefit constraint

$$\sum_{n=1}^{N}\sum_{i=1}^{I} m_{ni}AB_iC_i \geq CN \tag{13g}$$

(4) Planting area constraints

$$\sum_{n=1}^{N} m_{ni}A \geq A_{\min i},\ \forall i \tag{13h}$$

$$\sum_{n=1}^{N} m_{ni}A \leq A_{\max i},\ \forall i \tag{13i}$$

2.4. Spatial irrigation-water optimization

Based on the crop space planting structure, a GNFMP model was established to optimize irrigation-water allocation. Objectives of the GNFMP model include maximize economic benefits, maximize net irrigation-water productivity, and minimize blue water utilization. The meanings of the symbols can be found in Appendix I.

2.4.1. Objectives

(1) Maximize gross economic benefits:

Crop water production functions was approved to a useful tool for describing the relationship between yield of a certain crop and water resources (Smilovic et al., 2016). During the whole growth period, the crop water production function can be expressed as a quadratic function based on experimental data (Li et al., 2019c). The gross economic benefits can be expressed as follows:

$$\max F_1' = \sum_{n=1}^{N}\sum_{i=1}^{I} m_{ni}AB_i\left[a_i\left(\sum_{t=1}^{T} W_{nit}\right)^2 + b_i\sum_{t=1}^{T} W_{nit} + c_i\right] \tag{14a}$$

(2) Maximize irrigation-water productivity:

Irrigation-water productivity, the ratio of total crop yield to total irrigation-water, is used for measuring the production efficiency. The specific objective function can be expressed as follows.

$$\max F_2' = \frac{\sum_{n=1}^{N}\sum_{i=1}^{I} m_{ni}A\left[a_i\left(\sum_{t=1}^{T} W_{nit}\right)^2 + b_i\sum_{t=1}^{T} W_{nit} + c_i\right]}{\sum_{n=1}^{N}\sum_{i=1}^{I}\sum_{t=1}^{T} m_{ni}AW_{nit}/\lambda} \tag{14b}$$

(3) Minimize blue water utilization rate:

Blue water utilization rate is the ratio of total VWC_B to the total VWC. This objective can be expressed as:

$$\min F_3' = \frac{\sum_{n=1}^{N}\sum_{i=1}^{I}\sum_{t=1}^{T} m_{ni}VWC_{Bnit}}{\sum_{n=1}^{N}\sum_{i=1}^{I}\sum_{t=1}^{T} m_{ni}VWC_{nit}} \tag{14c}$$

2.4.2. Constraints

(1) Water supply constraint

$$\sum_{n=1}^{N}\sum_{i=1}^{I} m_{ni}AW_{nit} \le \lambda Q_t, \forall t \tag{14d}$$

(2) Food security constraints:

$$\sum_{i=1}^{I}\sum_{n=1}^{N} m_{ni}A\left[a_i\left(\sum_{t=1}^{T} W_{ni}\right)^2 + b_i\sum_{t=1}^{T} W_{ni} + c_i\right] \ge FD\cdot PO, \forall i_{\text{grain crops}} \tag{14e}$$

(3) Crop water requirements constraints:

$$\sum_{i=1}^{N} m_{ni}(W_{nit} + EP_{nt}) \ge \sum_{i=1}^{N} m_{ni}ET_{\text{min}nit} \qquad \forall n,t \tag{14f}$$

$$\sum_{i=1}^{I} m_{ni}(W_{nit} + EP_{nt}) \le \sum_{i=1}^{I} m_{ni}ET_{C\ nit} \qquad \forall n,t \tag{14g}$$

(4) Non-negative constraint

$$W_{nit} \ge 0, \qquad \forall n,i,t \tag{14h}$$

2.5. Model solution method

There are multi-objective, integer, nonlinear, and fractional programming in the DIMP and DNFMP models in this paper. Thus, the minimum deviation method is used for converting the multi-objective model into a single-objective model for solving multiple objectives (Li et al., 2019b). The specific steps are as follows:

Step 1 Model the GIMP.
Step 2 Transform each objective function into a model with minimized objective.
Step 3 Solve each objective separately to obtain the maximum and minimum values of each objective: $F_1^{\max}, F_1^{\min}, F_2^{\max}, F_2^{\min}, F_3^{\max}, F_3^{\min}$.
Step 4 Convert multiobjective to single-objective model by the following formula, and solve it to obtain the spatial crop planting structure:

$$\max = \frac{F_1^{\max} - F_1}{F_1^{\max} - F_1^{\min}} + \frac{F_2^{\max} - F_2}{F_2^{\max} - F_2^{\min}} + \frac{F_3^{\max} - F_3}{F_3^{\max} - F_3^{\min}} \tag{15}$$

Step 5 Input the results of the GIMP model to the GNFMP model, and then repeat Steps 2 to 4 to generate the spatial water allocation results.

3. Application

3.1. Study area

The Heihe River basin (37°50′-42°40′ N, 98°−101°30′ E) is the second largest inland river basin in China, located in the middle of the Hexi Corridor and the eastern part of Gansu Province, northwest China. It is divided by the Yingluo and Zhengyi Gorge hydrological station as three parts including upstream, midstream and downstream. The geolocation of the study area is shown in Fig. 2.

The study area is the middle reach of the Heihe River basin, which is one of the main food production areas in northwest China (Zhang et al., 2019b). The main crops of this region are field corn ($i = 1$), seed corn ($i = 2$), wheat ($i = 3$) and some economic crops ($i = 4$). The growth period of these crops is concentrated from April to September ($t = 1, 2 \ldots 6$, respectively). Both farmland area and the water consumption in the middle reach occupy over 80% of the Heihe River Basin. Due to high evapotranspiration (ET_0 is 1,453–2,351 mm) and low precipitation (60–280 mm) in the region, irrigation is the main source of water for crops, accounting for more than 90% of the total water consumption. Unreasonable use of the land and water resources lead to too much water used in the middle reach, destroying the basin ecological environment (Zhang et al., 2019a). It is urgent for the middle reach of Heihe River Basin to find a more sustainable agricultural production strategy. Therefore, to improve the utilization efficiency of limited land and water resources, this study attempts to help regional managers optimally determine the main crop planting type for each grid ($A = 1$ km^2, $N = 2{,}150$) on cultivated land in the study area, and the amount of irrigation-water to each grid during different time periods.

The slope and aspect data (the spatial resolution is 90 m) of the study area come from the Geospatial Data Cloud (http://www.gscloud.cn/sources/). The elevation distribution (spatial resolution is 30 m) is derived from the ASTER GDEM data. The soil types (spatial resolution is 1 km) are from the Heihe Plan data management center (http://www.heihedata.org/). The distribution of aspect, slope, DEM, and soil type in the study area are shown in Fig. 3.

Fig. 3 indicates that the aspect and slope of the study area have high spatial variability. The DEM varies greatly between 1,234 m and 3,633 m above sea level, and the soil type is also very complex with 13 species. In this area, spatial crop planting structure and optimal water distribution are determined according to *CWR* and precipitation. However, *CWR* and precipitation are affected by many factors, such as terrain, soil, meteorological, and basic agricultural facilities (Tang et al., 2019). With the change of geographical location, these factors have high spatial variability. Remote sensing technology is considered as a potential tool to obtain spatial *ET* and precipitation information. According to actual conditions, two assumptions have been made in processing remote sensing data: 1) the soil water remains the same before and after the growth period (Allen et al., 1998); 2) due to the deep groundwater depth in study area, the groundwater recharge is negligible (Chadha and Chadha, 2007).

Deterioration of the ecological environment of the study area and limited water and soil resources jointly call for more precise allocation schemes in space. Thus, the RSM approach was applied to this area. In this process, several questions are desired to be solved: 1) high spatial variability exists in evapotranspiration and precipitation; 2) existing spatial resolution of remote sensing data is insufficient for practical resources planning problems; 3) few research efforts attempt to establish precise optimization models at a grid scale; and 4) conflicting objectives cannot be considered simultaneously in the decision-making process. To address the above problems, GIMP and GNFMP are developed to generate spatial decision-making alternatives for supporting decision makers in managing limited agricultural water and soil resources.

3.2. Data collection

This study selected 2014 as the typical year. The remote sensing data used in this paper were collected from the Global Precipitation

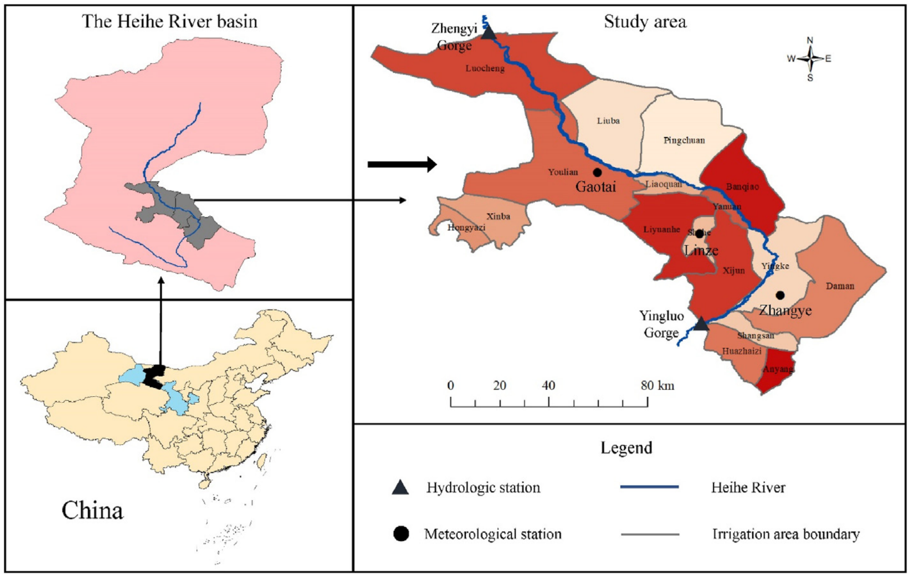

Fig. 2. Location of the study area.

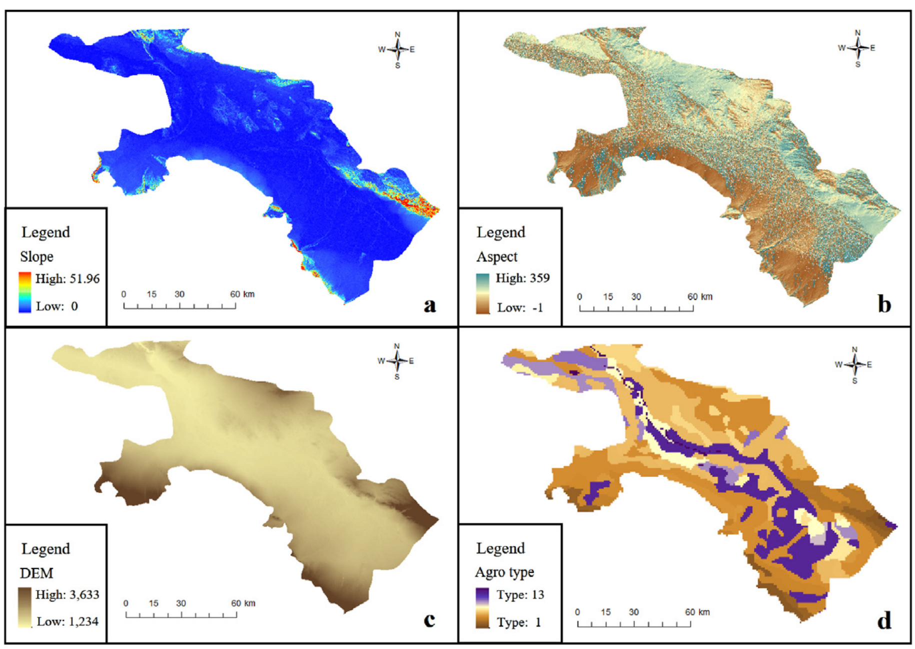

Fig. 3. Slope map (a), aspect map (b), DEM (c), and soil type map (d) in the study area.

Measurement (GPM) data (released on April 1st, 2014, spatial resolution is 0.1°, time resolution is month, Huffman et al., 2019), and MODIS/PET data (spatial resolution is 1 km, time resolution is month). Meteorological data were downloaded from the China Meteorological Data Service Center (http://data.cma.cn/en).

Socio-economic information, crop planting area, crop yield, water supply information, and hydrological information during 2004–2018 were collected from the Statistical Yearbook of Zhangye City and field research and trials. Irrigation-water production functions of different crops can be obtained from previous research (Li et al., 2017). Due to the priority position of economic crops, linear irrigation-water production functions is chosen for reflecting the relationship between irrigation-water and crop yield. The irrigation-water production function, market price, yield, and the available planting area of each crop are shown in Table 1.

K_C (crop coefficient) values of field corn, seed corn (Jiang et al., 2014), wheat (Kang et al., 2003) and economic crop (Li et al., 2019c) can be obtained from previous studies. The local population in 2014 was 82.07 × 10^4, the minimum grain demand per capital is 400 kg/per capital and the minimum gross economic benefit of the study area is determined according to the historic average net income per km^2, which is 110.61 × 10^8 CNY. K_C values, the monthly agricultural available groundwater, and surface water supply in the study area are shown in Table 2.

Through previous studies, the relationship between the ecosystem service value and the total crop planting area in this study area can be expressed as: $EV = \frac{49.21\times A-762.20}{A-15.56}$(Zhang et al.,

Table 1
Irrigation-water production function, market price, crop yield and available crop planting area.

Crop	Irrigation-water production function of crop (10^2 kg/km^2) (X is the amount of irrigation-water, cm)	Market Price (CNY/ kg)	Crop yield (10^4 kg/ km^2)	Available crop planting area (km^2)	
				Lower bound	Upper bound
Field corn	$Y = 3{,}281.67 + 199.83 \times X\text{-}1.22 \times X^2$	2.32	83.85	149.59	495.81
Seed corn	$Y = 3{,}604.24 + 179.58 \times X\text{-}1.23 \times X^2$	3.05	80.07	869.74	1,195.62
Wheat	$Y = 2{,}328.55 + 167.67 \times X\text{-}1.44 \times X^2$	2.26	84.39	195.97	267.31
Economic crop	$Y = -52{,}388.43 + 2099.00 \times X$	4.02	605.47	335.22	832.39

Table 2
K_C values of crops and the available water supply in each month.

Time	Kc value of main crops				Water supply (10^4 m^3)	
	Field corn	Seed corn	Wheat	Economic crop	Surface water	Ground water
April	0.20	0.22	0.30	0.51	3,837.53	2,342.30
May	0.44	0.50	1.15	0.86	15,618.13	2,366.09
June	0.53	1.16	1.15	1.03	23,341.89	2,335.39
July	1.46	1.20	0.93	1.05	30,835.91	2,351.78
August	1.14	1.20		0.64	28,765.76	2,335.12
September	1.22	0.60		0.62	14,925.84	2,291.28

2019b). The functional relationship between MOD16/PET and PM results is: $ET_0 = 0.7884 \times PET_{MOD16}$ - 28.3826 (Tang et al., 2019). The effective precipitation can be estimated by $EP = \alpha\cdot P$.

Where EV represents ecosystem service value, 10^8 CNY; A is the total crop planting area in study area, 10^4 ha; ET_0 is the reference crop evapotranspiration, mm; PET_{MOD16}, mm. EP is the effective precipitation, mm; $\alpha$is the effective precipitation coefficient, dimensionless. Based on previous studies, 0.8 was chosen for α in this area (Zhang et al., 2018); P is precipitation, mm.

The crop suitability data (spatial resolution is 1 km) of wheat (He et al., 2018), corn and economic crop (He et al., 2020) of this study area came from previous studies, which are shown in Fig. 4. The suitability of field corn and seed corn was not distinguished in collected data, and thus their suitability is assumed the same.

4. Results analysis and discussion

4.1. Results analysis and discussion of spatial basic data

4.1.1. Downscaling and accuracy analysis of precipitation

GPM data were released on April 1st, 2014, and the growth period of each crop in the study area is between April and June. Thus, this study uses the GPM data during the growth period from 2014 to 2018. The comparison of GPM data and ground observations is shown in Fig. 5 (a).

In Fig. 5 (a), a visible difference exists between the GPM data and the observation data, and the distribution is very scattered. Regression methods were used to fit the GPM data based on the ground observations, and the comparison results are shown in Fig. 5 (b). The deterministic coefficient (R^2, Gui et al., 2016) of these two data is 0.67, indicating that more accurate data are needed to meet the requirements in the optimization model. In order to further improve the accuracy of remote sensing information, the multiple linear regression method was used. Through the calculation, the regression equation can be obtained, which is shown in Equation (16). The corresponding MLR results are shown in Fig. 5 (c).

$$Y = 0.75*X_1 + 0.27*X_2 + 0.13*X_3 + 0.01*X_4 + 0.04*X_5 - 0.5*X_6 - 0.20 \quad (16)$$

Fig. 5 (c) shows that the R^2 of the multiple regression results have been improved to 0.80. The scatter distribution is more convergent, and the consistency between the predicted results and the actual results is improved. That is, when using remote sensing GPM data, terrain factors, and the geographic location information

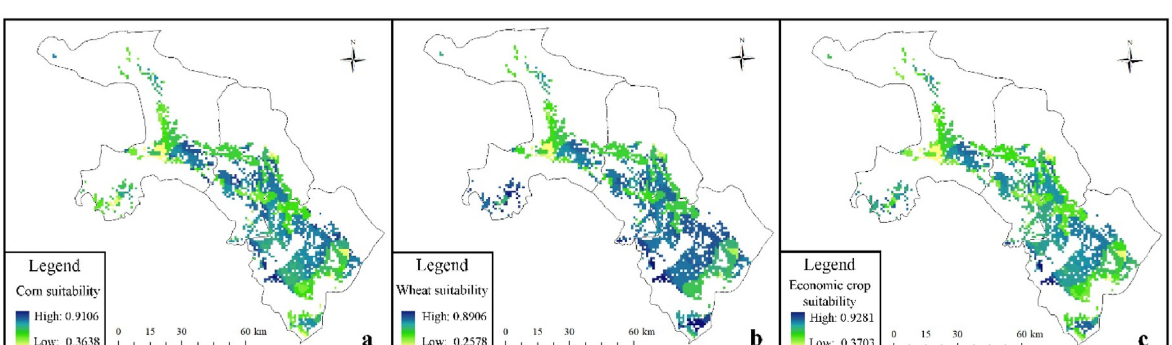

Fig. 4. Crop suitability in the middle reach of Heihe River basin.

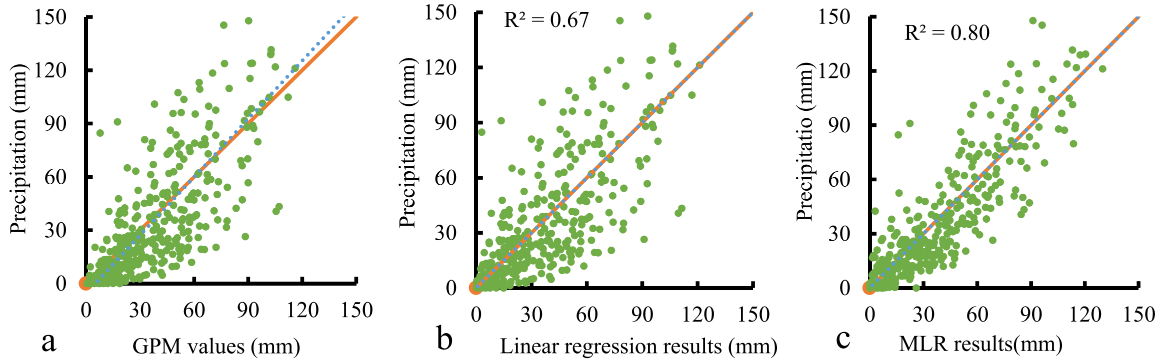

Fig. 5. Comparison of monthly ground observation precipitation with GPM values (a), the linear regression results (b) and the multiple regression results (c).

to obtain the spatial precipitation distribution results, the accuracy of results can be further improved. Then, MLRR results can be obtained after residual correction based on MLR results.

To verify the validity of the MLRR method, four datasets, including GPM, LR results, MLR results, and IDW results, were used for comparing with MLRR results through the cross-validation method. Three indicators, RMSE, MAE, and MRE, of each dataset can be calculated and are shown in Table 3. It is clear that the MLRR method has the best performance among these methods. MLRR can not only improve the accuracy of prediction results, but also help downscale the GPM to smaller grid (1 km $\times$ 1 km).

The final downscaling precipitation results (MLRR results) can be generated as Fig. 6 (b) (Taking the typical year of June as an example). Fig. 6 (a) shows the original GPM data with low spatial resolution (a). It can be found that the spatial resolution of the MLRR results has been improved, indicating that MLRR can help provide more precise data to meet the requirements of precise agricultural management. The MLRR results from April to September on cultivated land (Fig. 7) can be obtained in the same way. In Fig. 7, monthly precipitation obtained shows large spatiotemporal variability, and the areas with high precipitation are mainly mountainous areas near the upper reach. In summary, MLRR results can provide regional water managers more detailed information on a smaller scale. These information will be input to the DIMP and GNFMP models to determine crop planting structure and water allocation schemes.

4.1.2. *Results analysis and discussion of VWC*

Through a fitting function and MODD16/PET data, the monthly ET_0 results for each grid of cultivated field can be obtained as shown in Fig. 8, which have high spatiotemporal variability. According to the results obtained, the southern parts of the study area (closer to the upper reaches of the Heihe River Basin with higher elevation) featured as low potential evapotranspiration and high precipitation may be relatively humid, and thus have low irrigation-water demand. On the contrary, the northern parts (closer to the lower reaches of the Heihe River Basin with lower elevation) with high potential evapotranspiration and low precipitation are suffering in arid conditions, where irrigation plays a more important role in agricultural production. These information can obviously help regional managers formulate more sustainable agricultural production strategies to improve water use efficiency.

According to the virtual water theory, the monthly *VWC* of crops on each grid can be calculated. Fig. 9 shows accumulated *VWC* of each crop during whole growth period. The *VWC* values of the same crop in different grids have large gaps, and the *VWC* values of different crops in the same grid are also different. These spatiotemporal information will be considered in the RSM approach.

4.2. *Results analysis and discussion of DIMP model*

The optimization results of the GIMP model are shown in Fig. 10 (a). The total planted area obtained of field corn, seed corn, wheat, and economic crops are 393 km^2, 870 km^2, 267 km^2, and 396 km^2, respectively. To make a comparison with GIMP results, three single-objective models with objective F_1, F_2, and F_3, respectively, as well as the same constraints as GIMP were created. After solving these models, optimization results can be obtained as shown in Fig. 10(b and c, d). Optimization objectives of F_1, F_2, and F_3 each focus on one certain aspect, ignoring other important impacts. The GIMP model comprehensively considered all three objectives, and rational spatial distribution results can be obtained. As shown in Fig. 10, we found that: 1) economic crop are mainly concentrated in south areas, which may be caused by its high water demand and crop suitability; 2) the distribution of wheat relatively scattered in the study area, because the north with high potential evapotranspiration and low precipitation can save the limited water recourse, while its crop suitability is higher in the south; 3) field corn and seed corn are concentrated in the central region, where the crop suitability of these crops are higher than others; 4) seed corn has the greatest advantages and the largest planting area among all crops, which is consistent with its economic benefit and crop suitability performance; 5) areas with no allocated crop are mainly located in regions with high potential evapotranspiration, low

Table 3
RMSR, MAE, MRE and the ranking of GPM, LR, MLR, IDW, MLRR datasets.

Method	RMSE	Rank of RMSE	MAE	Rank of MAE	MRE	Rank of MRE
GPM	42.5827	4	34.3659	4	0.4609	5
LR	44.0797	5	35.2389	5	0.4551	4
MLR	28.4422	3	22.1755	3	0.4424	3
IDW	24.9587	2	20.9421	2	0.3695	2
MLRR	24.1615	1	18.0322	1	0.3688	1

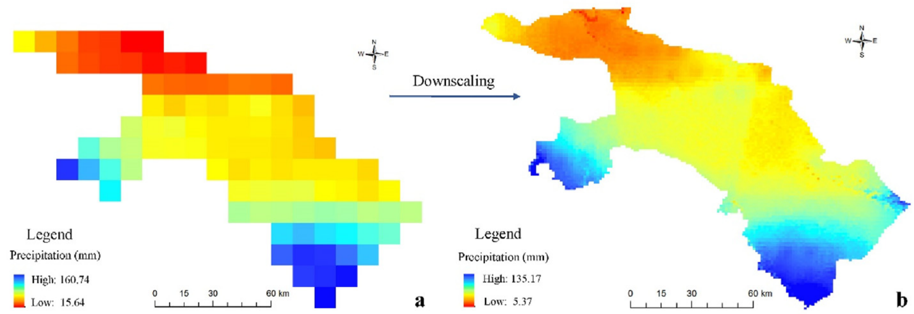

Fig. 6. GPM precipitation (a), and downscaling precipitation results (b) of June 2014.

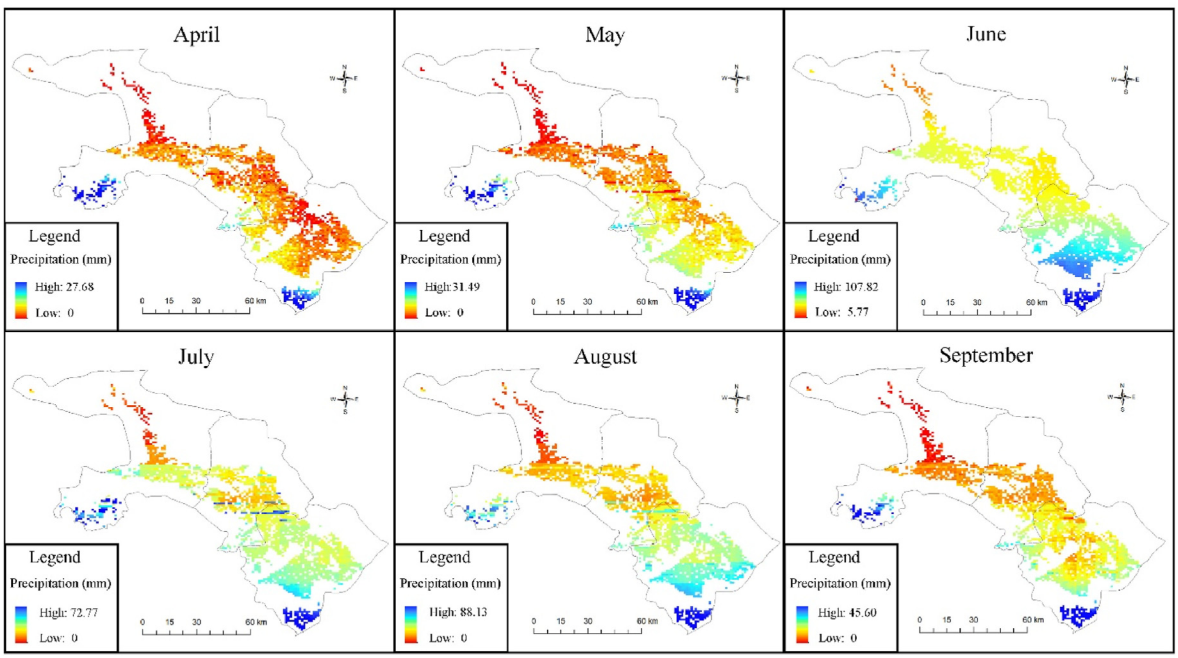

Fig. 7. The precipitation from April to September in typical year on cultivated land.

precipitation, and low suitability of all four crops. That is, if regional managers want to alleviate the pressure on the ecological environment in the study area, the areas with no allocated crop could be returned to forests to meet local policy requirements. Decision makers can determine the best planting location of each crop with the help of these results, and thus the utilization efficiency of land resources and system benefits can be improved.

As comparison made in Fig. 11, DIMP can provide suitable planting locations for seed and field corn, while the status quo can hardly provide such information. More economic crop should be planted to enhance the economic benefit of the agricultural system, especially in south areas with high suitability and low evaporation. DIMP results show that some areas should not be farmed when attempting to improve the total value of ecosystem services and ensure the grain output and economic benefits simultaneously.

Objective-value comparisons among these models have been made in Fig. 12. The objective values of the GIMP model are between the upper and lower values of the three single objective models, illustrating that the GIMP model can effectively manage tradeoffs among resources, efficiency and ecological objectives. The results can ensure current economic benefits and food security and reduce the total water demand. The ecosystem service value of the system can be increased by 0.36×10^8 CNY. These results will be input to the GNFMP model for optimizing spatial water allocation.

4.3. Results analysis and discussion of DNFMP model

Based on GIMP results and necessary spatial information, optimization results of monthly irrigation-water allocation can be calculated through the GNFMP model as Fig. 13 shows. The red area means that location has no irrigation-water allocation in the current month, which mainly are the areas with no crop planted in the GIMP model. The red area has a significant increasing trend in August and September because the wheat has been harvested in July. Results provide more detailed water allocation schemes of the whole basin, which cannot be obtained by previous optimization models. Regional managers can allocate the limited irrigation-water based on optimization results obtained to improve water use efficiency of the river basin.

To make comparisons with GNFMP results, three single-objective models with objectives F_1', F_2', and F_3' separately as well as the same constraints with GNFMP were created. The objective

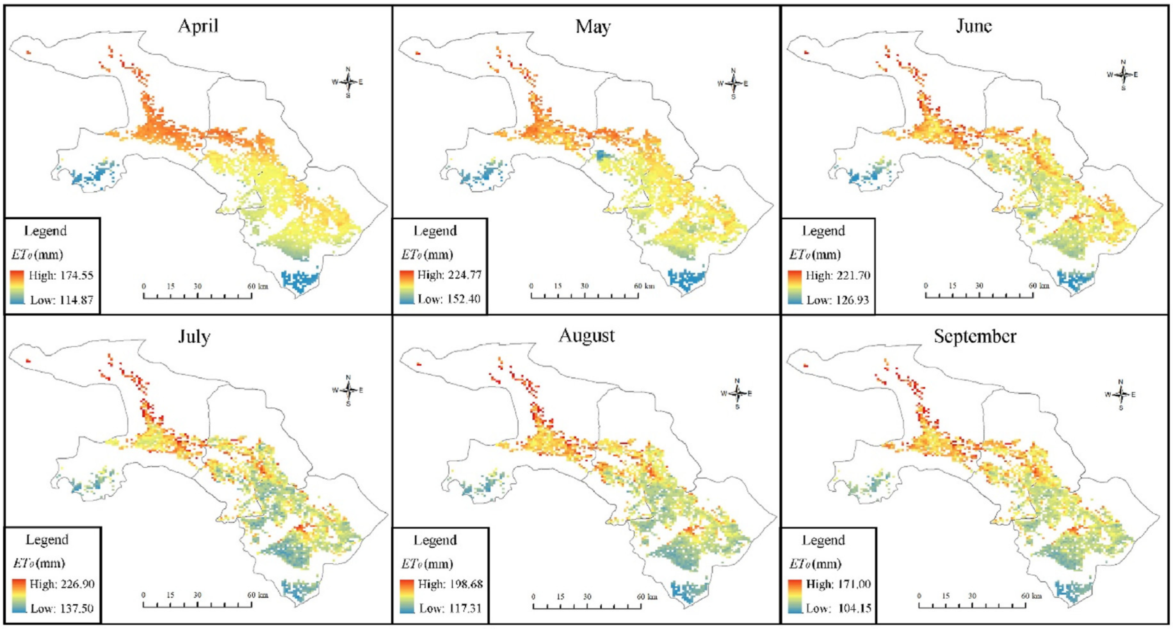

Fig. 8. Monthly ET_0 results on each grid for cultivated fields, 2014.

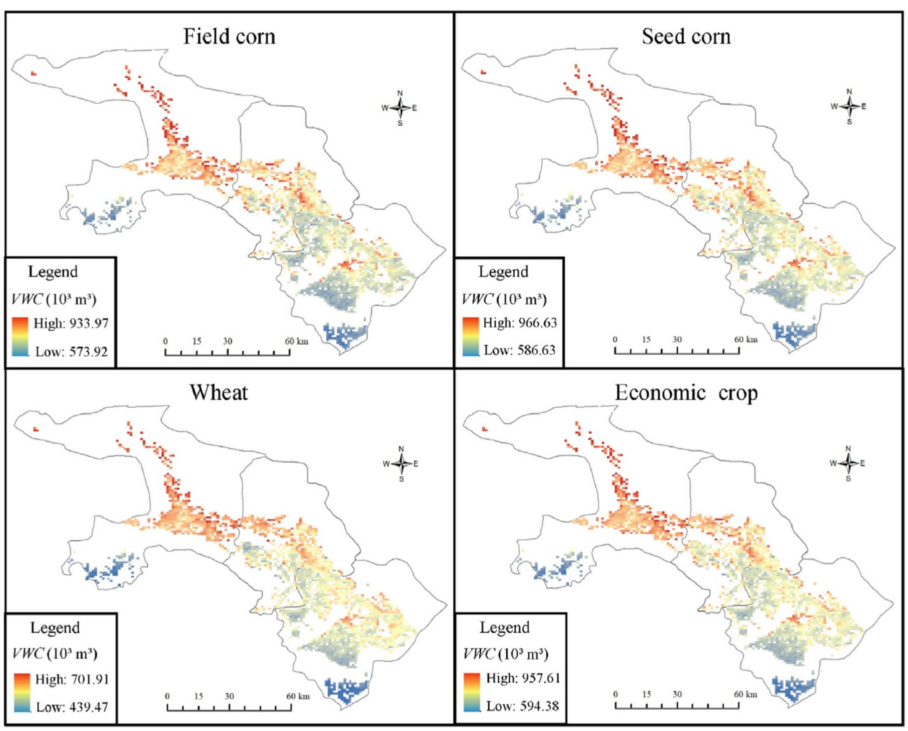

Fig. 9. *VWC* of each crop for each grid in 2014.

values of the GNFMP model, single-objective models, and current situation are shown in Fig. 14. It is noteworthy that each single objective model only obtain the best value in this objective, but perform poorly on others. The multiobjective model can manage tradeoffs among multiple objectives to obtain more reasonable results. Compared with the current situation, the GNFMP model improves the gross economic benefit of 24.17×10^8 CNY, increases the irrigation-water productivity of 0.50 kg/m^3, and reduces the blue water utilization rate by 0.18, indicating that results of the GNFMP model can effectively improve all objectives relative to the current situation and will contribute to agricultural systems management in river basins.

5. Conclusions

This study proposed a RSM approach for managing agricultural land and water resources in smaller spatial resolution. This approach coupled several remote sensing data sets to generate

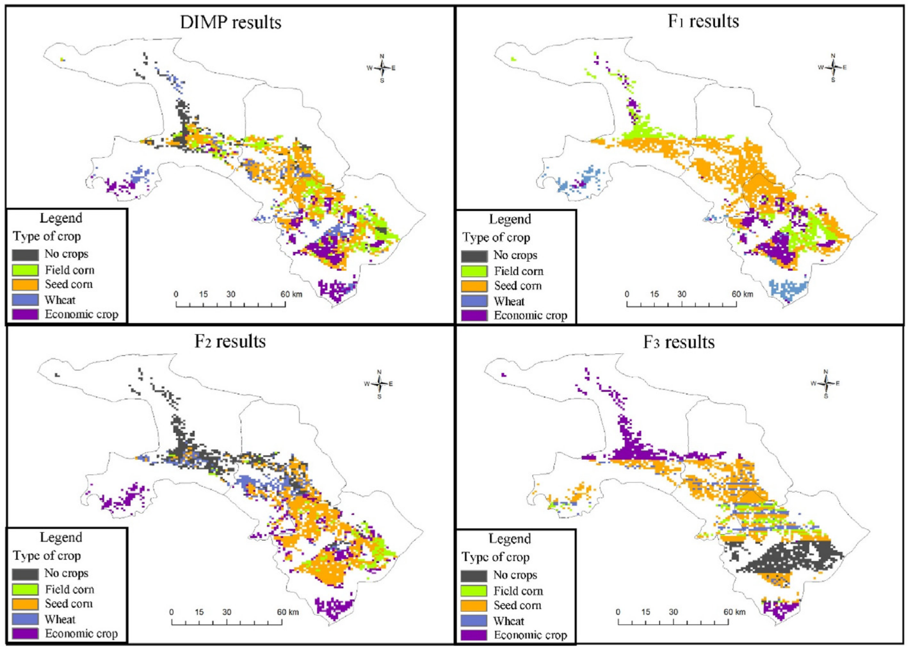

Fig. 10. Optimization results of spatial planting structure.

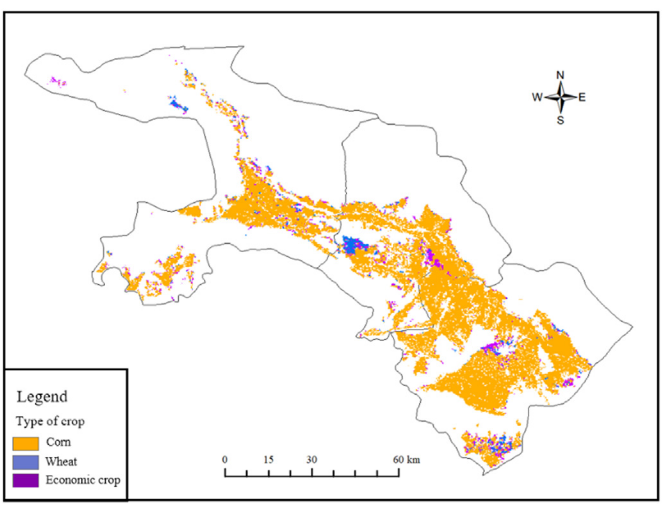

Fig. 11. Status quo of crop planting structure in 2014.

spatial downscaled data sets of GPM precipitation with the help of the MLRR method. Spatial *CWR* and *VWC* results can be calculated based on MOD16/PET data, PM mothed and virtual water theory. After getting these spatial data sets, GIMP model and GNFMP model were developed to generate optimal spatial crop planting structure and irrigation-water allocation schemes respectively. Decision makers can obtain more detailed spatial allocation schemes of agricultural land and water resources in river basins through RSM.

The main conclusions are as follows.

(1) The MLRR method for downscaling the GPM data sets has higher accuracy than LR, MLR, and IDW in precipitation prediction. The MLRR results show the high spatiotemporal variability in study area, which increased from north to south. The obtained spatial *VWC* results show that high spatiotemporal variability also exists in the *ET* and *VWC*, and decreased from north to south.
(2) GIMP results can help managers determine which crop are suitable for planting in all grids, and indicate that seed corn has the greatest advantages and the largest planting area.

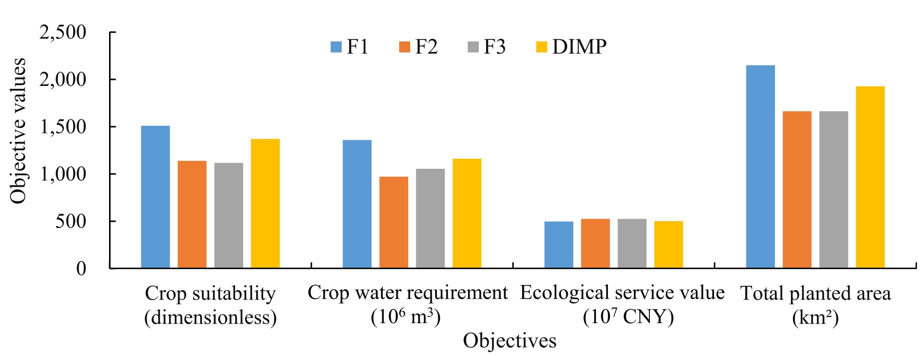

Fig. 12. The objective values of different optimization models in GIMP.

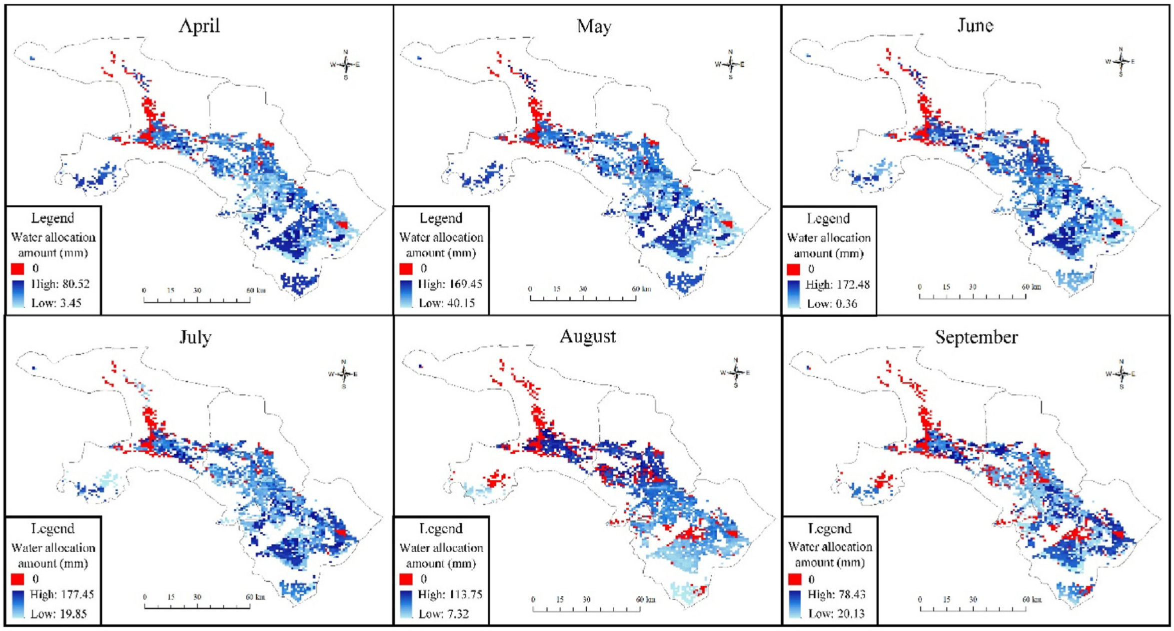

Fig. 13. Irrigation-water allocation in each month.

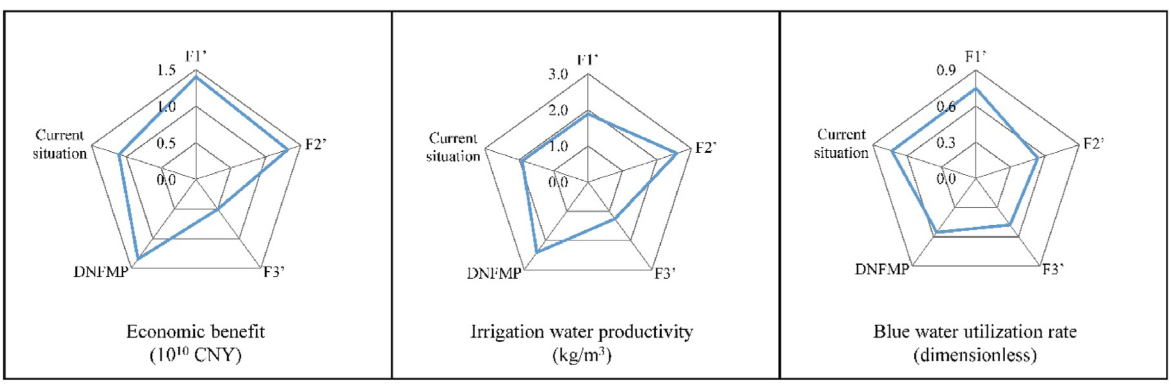

Fig. 14. The objective values of optimization models and status quo for the study area.

GIMP successfully managed tradeoffs among resources, efficiency, and ecological objectives, its results reduced the total water requirements and increased the ecosystem service value by 0.36×10^8 CNY.

(3) The grid-based water allocation results obtained from GNFMP effectively made tradeoffs among multiple objectives. Compared with the status quo, it improved the gross economic benefit by 21.85%, increased the irrigation-water productivity by 25.92%, and reduced blue water utilization rate by 24.32%.

RSM results can intuitively show the suitable crop planting type and optimal irrigation-water allocation on each grid, which is more practical for decision makers. The RSM approach proposed in this research can not only improve the spatiotemporal resolution and efficiency of agricultural systems, but also contribute to environmental restoration in the middle and lower reaches of the Heihe River. The study can also be applied to other similar regions. Some key factors, such as soil water, irrigation facilities and technology, regional policies haven't been fully considered in this study. A decision-making system can help these methods more accessible for practical managers, which will be considered as our future work.

Declaration of competing interest

The authors declare that they have no known competing financial interests or personal relationships that could have appeared to influence the work reported in this paper.

CRediT authorship contribution statement

Yikuan Tang: Conceptualization, Methodology, Formal analysis, Writing - review & editing. **Fan Zhang:** Conceptualization, Writing - review & editing. **Bernard A. Engel:** Writing - review & editing. **Xiao Liu:** Writing - review & editing. **Qiong Yue:** Writing - review & editing. **Ping Guo:** Resources, Writing - review & editing, Funding acquisition.

Acknowledgments

This research was supported by the National Natural Science Foundation of China (41871199, 51621061). The authors would extend the appreciation to anonymous reviews and editors for their comments and suggestions that significantly helpful in improving the quality of this paper.

Appendix I. Definitions of symbols used in DIMP and DNFMP models.

Indices, Variables, Objective functions, and Parameters Description.

	Definition
Indices	
N	Index of grid (i = 1,2, …,N)
I	Index of crop (i = 1,2, …,I)
T	index of period (i = 1,2, …,T)
max	Superscript of maximum
min	Superscript of minimum
Variables	
m_{ni}	The variables of whether to plant crops i for the grid n
W_{nit}	Net water allocation to the crop i for the grid n in period t (mm)
Objective functions	
F_1	Objective functions for system crop growth suitability (dimensionless)
F_2	Objective functions for spatial crop water requirements of system (m^3)
F_3	Objective functions for ecosystem service value (CNY)
F_1'	Objective functions for gross economic benefits (CNY)
F_2'	Objective functions for net irrigation-water productivity (kg/m^3)
F_3'	Objective functions for blue water utilization rate (dimensionless)
Parameters	
η_{ni}	Crop suitability of crop i for the grid n (dimensionless)
A	Area for each grid (km^2)
$ET_{C\ nit}$	Crop water requirement of crop i for grid n in period t (mm)
EP_{nt}	Effective precipitation for grid n in period t (mm)
EV	Ecosystem service value (CNY)
FD	Minimum grain demand per capital (kg/per capital)
PO	Population
B_i	Benefit per unit yield of crop i (CNY/kg)
C_i	Actual crop yield per unit area of crop i (kg/m^3)
CN	Current net profit of study area (CNY)
$A_{\min\ i}$	Minimum planting area of crop i
$A_{max\ i}$	Maximum planting area of crop i
a_i	Quadratic coefficient of crop water production function of crop i (dimensionless)
b_i	Primary coefficient of crop water production function of crop i (dimensionless)
c_i	Constant term of the crop water production function of crop i (dimensionless)
Q_t	Water supply for study area in period t (m^3)
λ	Proportion of agricultural water utilization of study area (dimensionless)
$ET_{min\ nit}$	Minimum water requirement for growth of crop i for grid n in period t (mm)
$VWC_{B\ nit}$	Blue water components of crop i for grid n in period t (mm)
VWC_{nit}	Virtual water content of crop i for grid n in period t (mm)

References

Abah, R.C., Petja, B.M., 2017. Crop suitability mapping for rice, cassava, and yam in North Central Nigeria. J. Agric. Sci. 9, 96–108.

Agnew, M.D., Palutikof, J.P., 2000. GIS-based construction of baseline climatologies for the Mediterranean using terrain variables. Clim. Res. 14, 115–127.

Allan, J., 1993. Fortunately there are substitutes for water: otherwise our hydro-political futures would be impossible. In: ODA, Priorities for Water Resources Allocation and Management. ODA, London, pp. 13–26.

Allen, R.G., Pereira, L.S., Raes, D., Smith, M., 1998. Crop evapotranspiration: guidelines for computing crop water requirements. In: Food and Agriculture Organization. FAO Irrigation and Drainage, Rome, Italy. Paper No. 56.

Bastiaanssen, W.G.M., Molden, D.J., Makin, I.W., 2000. Remote sensing for irrigated agriculture: examples from research and possible applications. Agric. Water Manag. 46, 0-155.

Caselles, V., Delegido, J., Sobrino, J.A., Hurtado, E., 1992. Evaluation of the maximum evapotranspiration over the La Mancha region, Spain, using NO A A AVHRR data. Int. J. Rem. Sens. 13 (5), 939–946.

Chadha, S.S., Chadha, V., 2007. Linear fractional programming and duality. Cent. Eur. J. Oper. Res. 15 (2), 119–125.

Chen, T., Ren, L., Yuan, F., Yang, X., Jiang, S., Tang, T., Liu, Y., Zhao, C., Zhang, L., 2017. Comparison of spatial interpolation schemes for rainfall data and application in hydrological modeling. Water 9, 342.

Chono, S., Maeda, S., Kawachi, T., Imagawa, C., Buma, N., Takeuchi, J., 2012. Optimization model for cropping-plan placement in paddy fields considering agricultural profit and nitrogen load management in Japan. Paddy Water Environ. 10, 113–120.

Fasakhodi, A.A., Nouri, S.H., Amini, M., 2010. Water resources sustainability and optimal cropping pattern in farming systems; a multi-objective fractional goal programming approach. Water Resour. Manag. 24, 4639–4657.

Goovaerts, P., 2000. Geostatistical Approaches for incorporating elevation into the spatial interpolation of rainfall. J. Hydrol 228, 113–129.

Gui, Z., Li, M., Guo, P., 2016. Simulation-based inexact fuzzy semi-infinite programming method for agricultural cultivated area planning in the Shiyang River Basin. J. Irrigat. Drain. Eng. 143 (2), 5016011.

He, L., Bao, J., Daccache, A., Wang, S., Guo, P., 2020. Optimize the spatial distribution of crop water consumption based on a cellular automata model: a case study of the middle Heihe River basin, China. Sci. Total Environ. 720, 137569.

He, L., Wang, S., Peng, C., Tan, Q., 2018. Optimization of water consumption distribution based on crop suitability in the middle reaches of Heihe River. Sustainability 10, 2119.

Hoekstra, A.Y., Chapagain, A.K., Mekonnen, M.M., Aldaya, M.M., 2011. The Water Footprint Assessment Manual: Setting the Global Standard. Earthscan, London.

Huffman, G.J., Stocker, E.F., Bolvin, D.T., Nelkin, E.J., Tan, Jackson, 2019. GPM IMERG Final Precipitation L3 1 Month 0.1 Degree X 0.1 Degree V06, Greenbelt, MD. Goddard Earth Sciences Data and Information Services Center (GES DISC), Accessed: [Data Access Date], 10.5067/GPM/IMERG/3B-MONTH/06.

Immerzeel, W.W., Rutten, M.M., Droogers, P., 2009. Spatial downscaling of TRMM precipitation using vegetative response on the Iberian Peninsula. Remote Sens. Environ. 113, 362–370.

Jiang, X., Kang, S., Tong, L., Li, F., Li, D., Ding, R., Qiu, R., 2014. Crop coefficient and

evapotranspiration of grain maize modified by planting density in an arid region of northwest China. Agric. Water Manag. 142, 135–143.
Kang, S., Gu, B., Du, T., Zhang, J., 2003. Crop coefficient and ratio of transpiration to evapotranspiration of winter wheat and maize in a semi-humid region. Agric. Water Manag. 59, 239–254.
Li, K., Huang, G., Wang, S., 2019a. Market-based stochastic optimization of water resources systems for improving drought resilience and economic efficiency in arid regions. J. Clean. Prod. 233, 522–537.
Li, M., Fu, Q., Guo, P., Singh, V.P., Zhang, C., Yang, G., 2019b. Stochastic multi-objective decision making for sustainable irrigation in a changing environment. J. Clean. Prod. 223, 928–945.
Li, M., Fu, Q., Singh, V.P., Ji, Y., Liu, D., Zhang, C., Li, T., 2019c. An optimal modelling approach for managing agricultural water-energy-food nexus under uncertainty. Sci. Total Environ. 651, 1416–1434.
Li, M., Fu, Q., Singh, V.P., Liu, D., Li, T., 2019d. Stochastic multi-objective modeling for optimization of water-food-energy nexus of irrigated agriculture. Adv. Water Resour. 127, 209–224.
Li, M., Jiang, Y., Guo, P., Li, J., 2017. Irrigation water optimal allocation considering stakeholders of different levels. Trans. Chin. Soc. Agric. Mach. 48 (5), 199–207 (in Chinese).
Michaelides, S., Levizzani, V., Anagnostou, E., Bauer, P., Kasparis, T., Lane, J.E., 2009. Precipitation: measurement, remote sensing, climatology and modeling. Atmos. Res. 94, 0-533.
Mu, Q., Heinsch, F.A., Zhao, M., Running, S.W., 2007. Development of a global evapotranspiration algorithm based on MODIS and global meteorology data. Remote Sens. Environ. 111, 519–536.
Smilovic, M., Gleeson, T., Adamowski, J., 2016. Crop kites: determining crop-water production functions using crop coefficients and sensitivity indices. Adv. Water Resour. 97, 193–204.
Su, X., Li, J., Singh, V.P., 2014. Optimal allocation of agricultural water resources based on virtual water subdivision in Shiyang River Basin. Water Resour. Manag. 28, 2243–2257.
Tang, Y., Zhang, F., Wang, S., Zhang, X., Guo, S., Guo, P., 2019. A distributed interval nonlinear multiobjective programming approach for optimal irrigation water management in an arid area. Agric. Water Manag. 220, 13–26.
Velpuri, N.M., Senay, G.B., Singh, R.K., Bohms, S., Verdin, J.P., 2013. A comprehensive evaluation of two MODIS evapotranspiration products over the conterminous United States: using point and gridded FLUXNET and water balance ET. Remote Sens. Environ. 139 (4), 35–49.
Westerhoff, R.S., 2015. Using uncertainty of Penman and Penman–Monteith methods in combined satellite and ground-based evapotranspiration estimates. Remote Sens. Environ. 169, 102–112.
Zhang, F., Guo, S., Zhang, C., Guo, P., 2019a. An interval multiobjective approach considering irrigation canal system conditions for managing irrigation water. J. Clean. Prod. 211, 293–302.
Zhang, F., Yue, Q., Engel, B.A., Guo, S., Guo, P., Li, X., 2019b. A bi-level multiobjective stochastic approach for supporting environment-friendly agricultural planting strategy formulation. Sci. Total Environ. 693, 133593.
Zhang, F., Zhang, C., Yan, Z., Guo, S., Wang, Y., Guo, P., 2018. An interval nonlinear multiobjective programming model with fuzzy-interval credibility constraint for crop monthly water allocation. Agric. Water Manag. 209, 123–133.